Affinity-selected peptide ligands specifically bind i-motif DNA and modulate c-Myc gene expression

Summer Rosonovski,[1Y] Dilek Guneri,[2Y] Jessica King,[3] Christoper J. Morris.[2]*, and Zoë A. E. Waller,[2]*

1. School of Pharmacy, University of East Anglia, Norwich Research Park, Norwich, NR4 7TJ, UK.
2. UCL School of Pharmacy, 29-39 Brunswick Square, London, WC1N 1AX, UK.
3. Pharmaceutical and Biological Chemistry, University of Western Australia, Crawley, Australia.

[Y] These authors contributed equally to this work.

Abstract

c-Myc is an oncogene that is dysregulated in ~70% of cancers. Its multifaceted function complicates effective drug targeting of the protein. i-Motif DNA structures in gene promotor regions have gained attention for their potential role in modulation of gene expression. These include the i-motif formed by the cytosine-rich sequence that lies upstream of the key P1 promotor of the c-Myc gene. Currently, selective ligands interacting with i-motif structures are limited. Here, peptide ligands for the i-motif from the promoter of c-Myc were identified *via* phage display. Hit peptides were filtered for selective binding to i-motif structures over other DNA structures using displacement assays and DNA melting experiments. Two lead peptides were found to produce dose-dependent changes on c-Myc gene expression after delivery into HEK293 cells expressing a c-Myc luciferase reporter construct. These leads may be used as chemical tools for the manipulation of c-Myc i-motif *in vitro* and have potential to be developed into cell-permeable peptidomimetics for delivery *in vivo*.

Introduction

i-Motifs (iMs) are non-canonical nucleic acid secondary structures formed from cytosine-rich sequences, zipped together through hemi-protonated cytosine-cytosine base pairs.[1, 2] iM-forming sequences are well-characterized to be able to form *in vitro* at neutral pH[3, 4] and have been shown to be present and involved in transcription and proliferation, in cells.[5-7] More recently, there have been reports of iM-binding small molecules, but selectivity remains an issue for iM ligands. Indeed, many G-quadruplex (G4) binding ligands have also been found to interact with diverse iM structures. Consequently, the discovery of specific iM-binding ligands is crucial to develop both target-specific chemical tools and future therapeutics.

The proto-oncogene, c-Myc, is a multifunctional transcription factor which controls various downstream genes and coordinates a range of cellular processes in both health and disease.[8] Elevated expression of c-Myc in cancer occurs through several mechanisms (e.g. gene amplification, chromosomal translocation) and results in elevated tumour aggression and poorer clinical outcomes.[9] Substantial experimental evidence has established that reducing overactive c-Myc can lead to cancer regression.[8, 10-12] One approach to direct targeting of the Myc protein is achieved by interference of the Myc-Max heterodimerisation. The peptide/protein candidates, OMO-103 and IDP-121, have progressed to Phase I clinical testing. OMO-103 dose-escalation trial results indicate that this is a tractable approach that can deliver anti-tumour activity across different tumor types.[13] A significant challenge for all protein/peptide-based drugs is the requirement to deliver an intracellular dose that is sufficient to neutralize all copies of the c-Myc protein in a cancer cell. These have been estimated to number 30,000 copies per cell.[14] Reports of siRNA-mediated knockdown of c-Myc mRNA levels indicate that this approach has merit, yet efficient intracellular delivery of siRNA can be similarly challenging and inefficient. A contrasting and arguably more potent approach involves targeting the c-Myc gene directly such that MYC levels are suppressed pre-transcriptionally through blockade of key protein-DNA promoter interactions. This approach is particularly appropriate considering the short half-life of both c-Myc mRNA (10 minutes) and protein (20 minutes).[15]

c-Myc transcription is largely controlled by the P1 and P2 promoter sites.[16] Upstream of the P1 promoter regulatory region there is a nuclease hypersensitivity element (NHE)-III_1 that is prerequisite for approximately 90% of c-Myc gene transcription.[17-19] This element contains GC-rich sequences capable of forming an iM, with a G4 on the complementary strand. G4 formation within the NHE III_1 region has been extensively studied, showing that destabilizing G4 structure leads to increased c-Myc transcription and stabilizing the G4 repressed transcription.[20-22] c-Myc transcription is proposed to be initiated by the negative supercoiling of the NHE-III_1 region that facilitates the G4 formation and creates a transient single-stranded region recognizable for elements of the transcription machinery. This may include helicases able to resolve the G4 structure and promote c-Myc expression.[23] However, negative supercoiling alone may not be the key mechanism to facilitate G4 formation.[24] Further insights into the regulatory region of the c-Myc promotor region are required to facilitate the development of novel ligands and potential drugs. This includes exploring the potential of iM-formation on the opposing strand.[25] [25]

Specific nucleoproteins have been found to bind iMs or G4s and subsequently modulate gene expression levels. Heterogeneous nuclear ribonucleoprotein K (hnRNP-K) is an RNA/DNA binding protein that binds to single-stranded, cytosine-rich sequences. It was shown by

Hurley and co-workers to bind and unfold the iM-forming sequence of c-Myc and to increase c-Myc transcription.[26] This was indirectly validated by others who observed that hnRNP-K gene-knockdown reduced MYC protein levels.[27]

Drawing inspiration from the binding activity of nucleoproteins, we aimed to identify peptidic ligands that could regulate quadruplex biology. Unlike non-selective small molecules and large antibody species, these peptide ligands would occupy a molecular size niche with potential for increased specificity compared to small molecules and improved intracellular delivery capabilities compared to antibodies. Here, we deployed phage display to select 12-mer peptide ligands that bind selectively to the iM structure in the c-Myc promotor.

Materials and Methods

Chemicals were purchased from Sigma Aldrich/Merck, were of analytical or molecular biology grade and used without further purification.

Oligonucleotides (listed in Tables S1, S2) were purchased from Eurogentec and were RP-HPLC purified. Solid DNA samples were initially dissolved in ultrapure water to a concentration of 1 mM. Stock concentrations were confirmed using the extinction coefficients provided by Eurogentec and their UV absorbance at 260 nm with a Nanodrop ND-1000 spectrophotometer. The samples were prepared as 10 µM DNA in 10 mM sodium cacodylate (NaCaco) buffer at pH 6.6 and thermally denatured at 95 °C for 5 minutes and allowed to anneal slowly to room temperature overnight.

Phage display of peptides and c-Myc i-motif ligand selection. The NEB Ph.D.TM-12 library, containing ca. 109 randomized, linear 12-mer peptide sequences was panned against c-MycC52 i motif following the protocol described in the NEB Phage Display instruction manual. Key buffers used in the library panning were: Incubation buffer (PBS pH 6.0), wash buffer (PBS pH 6.0 with 0.01-0.05% Tween 20), blocking buffer (PBS pH 6.0 with 5 mg/mL BSA), and elution buffer (PBS, pH 7.4) (Table S3).2 Phage display library panning involved solution-phase panning with a 5′-biotinylated c-MycC52 target and target capture on High-Capacity Streptavidin coated plates. PBS was the DNA buffer of choice for phage display as has a good buffering range across pH 5.8-7.4. c-MycC52 is unfolded at pH 7.4, fully folded at pH 5.8, and 50% folded at pH 6.44 (Figure S1). PBS pH 6.0 was chosen as the incubation buffer as this is slightly more acidic than the transitional pH of c-MycC52 in PBS (Figure S1). Table S3 summarises the three rounds of phage display screening that were undertaken. Target c-Myc C52 oligonucleotide was used alone in round one. Unbiotinylated competitor oligonucleotides were used in rounds two and three at the concentrations indicated in Table S3. At the end of each screening round phage were enumerated by titration with E. coli ER2738 and amplified in E. coli ER2738 as per NEB's phage display manual. At the end of round three, twenty-five individual phage plaques were harvested from IPTG/X-Gal plates and amplified on a 5 ml scale for 4 hours. ssDNA was isolated after iodide denaturation and ethanol precipitation. DNA sequenced using Sanger sequencing (Mix2Seq Eurofins) using the -96 gIII sequencing primer provided by NEB.

Peptides were purchased from Cellmano Biotech (Hefei, China) as RP-HPLC purified (> 95%) with N-terminal acetylation and C-terminal amidation to mimic the phage-displayed fusion peptides. Stock solutions of the peptides were made at 5 mg/mL in ultrapure water or DMSO (if water insoluble) and were stored at −20 °C. Subsequent dilutions were made in the appropriate assay buffer. Stock concentrations were confirmed using the peptide extinction coefficients and UV absorbance on Agilent Technologies Cary 4000 UV-VIS spectrometer. The Nick Anthis' Protein Parameter Calculator was used to find the extinction coefficient either at 280 nm if the sequence contained any tryptophan or tyrosine residues or at 205 nm if the sequence contained neither of these amino acids.[28]

Fluorescent Indicator Displacement (FID) experiments used in this publication are based on the first FID assay developed for i motif DNA.[29] The FID experiments were performed on a BMG CLARIOstar plate reader using 96-well, solid black flat bottom plates. Thiazole Orange (TO) was the indicator, and the stock solution was prepared at 10 mM in DMSO. The TO stock was diluted into the appropriate buffer to 2 µM. Each well had 9 µL of the 2 µM TO solution added and excited at 430 nm with fluorescence emission at 450 nm measured; this was normalized to 0% to account for background fluorescence. 1 µL of 90 µM DNA was added to each well and shaken in the plate reader for 30 seconds using double orbital shaking at 700 rpm and left for 10 minutes to equilibrate. Following equilibration, fluorescence emission was measured and normalized to 100% representing maximum fluorescence. Peptides were titrated in 25 µM in 0.9 µL additions until 200 µM into each well in triplicate until 200 µM of peptide was reached, and fluorescence emission was measured following each addition. Fluorescence emission for each well was normalized between 0 and 100% which was taken away from 100 to give the percentage of displacement. The data was analyzed in Origin data analysis software and fitted with a hyperbolic dose-response curve from which the DC_{50} value was interpolated.

Circular Dichroism (CD) melting experiments were performed in Jasco J-1500 spectropolarimeter with 10 µM DNA samples in 10 mM sodium cacodylate buffer at pH 6.6 using a 1 mm path length quartz cuvette. Initially two repeats of CD melting full spectrum ranges were taken (from 230 nm to 320 nm) for c MycC27, c-MycC52, c-MycG27, c-MycG52, and dsDNA (Table S1) measuring the unfolding of the DNA structures from 5°C - 95°C in presence of 10 molar equivalent DMSO, Pep-PTN or Pep VSE as well as Pep-SLC and buffer for dsDNA. The samples were kept at 5°C for 5 minutes before starting the melt with 1°C/min increase in temperature, 0.5°C data interval and 60 seconds holding time at each target temperature. Four scans were accumulated data pitch at 0.5 nm, scanning speed of 200 nm/min, 1 second response time, 2 nm bandwidth, and 200 mdeg sensitivity. Furthermore, two CD melting experiment repeats were performed recording C-rich c-Myc at 288 nm and 320 nm, G-rich c-Myc at 264 nm and 320 nm, and dsDNA at 253 nm and 320 nm with the settings as described for full spectrum measurements. Data was zero corrected to 320 nm and baseline drift. The melting temperature (T_M) was concluded using the Boltzmann fitting curve on the folded fraction data using GraphPad Prism version 10.1.2. Data was processed as Mean ± SEM (n=4) and One-way ANOVA followed by Bonferroni post-hoc test to determine significant changes between peptides and controls.

Cell Studies. HEK293 cells (ATTC CRL-1573 ™) at passages 30 were cultivated in DMEM medium supplemented with 10% FBS (Gibco, UK) and passaged at 80% confluency every 3-4 days under standard cell culture conditions. Cells from passage 32-38 were seeded in 6 well plates at 1x105 cell density/well in DMEM medium with 10% FBS. Once 80% confluency is reached the cells were co-transfected with c Myc promoter (Del-4) Firefly luciferase plasmid gifted by Bert Vogelstein (Addgene plasmid # 16604; http://n2t.net/addgene:16604; RRID:Addgene_16604)9 and control Renilla reporter vector (Promega, pRL-TK Vector GenBank® Accession Number AF025846) at 3:1 ratio. The plasmid mix and Lipofectamine TM 2000 (Invitrogen, UK) were prepared in a 1:1 ratio and incubated for 15 minutes at RT. The following day, cells were seeded in a white 96 well plate and a transparent 95 well plate (Greiner, Germany) at 5x104 cell density/well in DMEM medium with 2% FBS. The following day, both plates were treated simultaneously with three technical repeats of transfected HEK293 cells were treated with of 1 µM, 5 µM and 10 µM Pep-PTN or Pep-VSE or 0.2% DMSO control using Nanocin PRO (TECREA, UK) as peptide delivery vehicle. The transparent 96 well plate was, in addition, treated with 20 µL CellTiter 96® Aqueous One Solution for cell proliferation assay (Promega, USA). After 4h of peptide treatment, the cell proliferation was determined by measuring absorbance at 490 nm, subtracting blank measurements without cells, and normalized to DMSO-treated cells. The cells in the white 96 well plate was used for the Dual Luciferase Reporter Assay (Promega, USA) to determine the c Myc promotor activity. The Firefly-based bioluminescence and normalized to Renilla-based signals and normalized for 0.2% DMSO control-treated cells. Both assays were measured using the SpectraMax iD3 (Molecular Devices, UK). GraphPad Prism version 10.1.2. was used to determine Mean ± SEM and One-way ANOVA followed by Bonferroni post-hoc test of six biological repeats both cellular studies.

Results and Discussion

Phage display is a recombinant screening technique that permits the rapid screening of libraries with diversity up to 10^9 unique ligand peptides or antibody fragments against a given target such as iM and G4 structures.[5, 30] We screened a 12-mer linear peptide library against the biotinylated 52 bp C-rich c-Myc promoter sequence (c-MycC52, 5′-CTT-CTC-CCC-ACC-TTC-CCC-ACC-CTC-CCC-ACC-CTC-CCC-ATA-AGC-GCC-CCT-CCC-G-3′) that has been shown to be necessary for effective transcriptional firing from the P1 and P2 promoters.[26, 31] The selection pressure for each round of panning was increased by adding non-biotinylated competitor DNA sequences (Table S2,S3). The five most abundant peptides were identified after three successive screening rounds, and their sequences were elucidated via DNA sequencing (Table 1).

Table 1. Top five most abundant 12-mer peptide sequences. Conserved sequence shown in bold; consensus sequence underlined.

Peptide Ligand	*Amino acid sequence*
Pep-EIE	EIEY**TDHMK**ELG
Pep-PTN	PTNVSGRNYLFC
Pep-RVS	RVS**TDHMK**GRGG
Pep-SLC	SLCDIIRIEKVR
Pep-VSE	VSEAWKEVKGFF

The most enriched peptide was Pep-EIE, which shared a TDHMK motif with Pep-RVS. Three peptides contained the consensus sequence: (S/T)(D/E)XX^2X^3 where X is any amino acid, X^2 is a large amino acid and X^3 is a basic amino acid. Pep-SLC included the closely related sequence, DIIR. Pep-PTN and Pep-SLC both included at least one arginine residue, which are typically depleted in the particular phage display library used.[40] Conventionally, arginine residues favor binding to pyrimidine-rich DNA regions, as evidenced by the abrogated binding of NM23-H2 to single stranded DNA after the substitution of a key arginine for alanine, reducing interactions with the phosphodiester backbone.[32]

The relative binding of the five peptide ligands to the folded c-MycC52 iM were assessed via a fluorescent indicator displacement (FID) assay[26] using thiazole orange (Fig. 1).

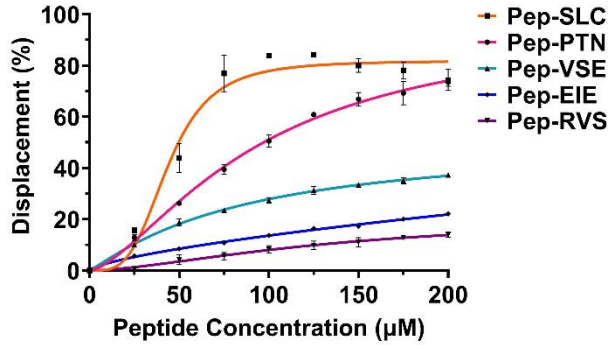

Figure 1. Concentration-dependent interaction of peptide with c-MycC52 i-motif determined via FID assay**.** The assay was performed with 1 µM c-MycC52 in 10 mM Sodium Cacodylate, pH 6.6, in the presence of 2 µM thiazole orange. Peptide ligands were added in increments of 25 µM up to a final concentration of 200 µM. Data are presented as Mean ± SD (n=3) and fitted using a Hill-Slope dose-response curve.

All five peptides demonstrated concentration-dependent intercalator displacement from the c-MycC52 iM. However, Pep-EIE and Pep-RVS displaced <20% of thiazole orange and showed no sign of plateau at 200 µM. The relative binding affinity was ranked as SLC>PTN>VSE>EIE>>RVS, with average displacement values at 100 µM spanning 5-85%. Pep-EIE and Pep-RVS were excluded from further analysis due to the poorer relative displacement capability of thiazole orange from the folded c-MycC52 iM structure.

To determine the effects of peptide binding on iM stability we measured DNA melting points (T_M) using circular dichroism (CD)-based melting experiments. The three remaining peptides were initially tested for off-target binding to double stranded (ds) DNA. Pep-SLC destabilized dsDNA by 5°C (Fig. S2A). Pep-PTN and Pep-VSE had no effect on dsDNA melting compared to the solvent controls (Fig. S2B), prompting us to exclude Pep-SLC from further consideration. Therefore, we tested the thermal stability of c-MycC52 iM and a shorter analogue c-MycC27 (5′-CCT-TCC-CCA-CCC-TCC-CCA-CCC-TCC-CCA-3′) (Fig. S3) as well as their complementary G4-forming sequences (c-MycG52 5′- CGG-GAG-GGG-CGC-TTA-TGG-GGA-GGG-TGG-GGA-GGG-TGG-GGA-AGG-TGG-GGA-GAA-G -3′) and c-MycG27 (5′- TGG-GGA-GGG-TGG-GGA-GGG-TGG-GGA-AGG3′) respectively in Fig. S4, in the presence of 10 molar equivalents of Pep-PTN or Pep-VSE. The stabilization temperatures are summarized in Table S5 and full meting curves are shown in Fig. S3, S4.

Both c-MycC27 and c-MycC52 sequences exhibited a double transition in the CD melts, implying two folded populations with different stabilities (Fig. S3). This was not unexpected, as both sequences have the capabilities of folding into different structures because of their length.[39] We determined the T_Ms of both species due to the likely existence of both iM topologies *in vivo*. The c-MycC27 and c-MycG27 sequences were neither stabilized nor destabilized by Pep-PTN nor PEP-VSE (Table 2, and Fig. S3A,B & Fig S4A,B). In contrast, the peptides significantly modulated the thermal stability of the biologically relevant c-MycC52 and the complementary G-rich sequence (p<0.001***). Specifically, both iM populations formed by c-MycC52 showed significant destabilization in presence of Pep-VSE (Table 2, Figs. S3C, S3D). Interestingly, the T_M decrease of the c-MycC52 sequence was greater for the more stable iM population, with a ΔT_M of -14±0.5°C (p<0.001***, see Fig S3D).

Table 2. CD melting analysis of 10 µM c-MycC27 and c-MycC52 and their complimentary c-MycG sequences in 10 mM Sodium Cacodylate at pH 6.6 buffer in the presence of 10 molar equivalents of Pep-PTN, Pep-VSE or the DMSO solvent control. All data are presented as Mean change in the higher Tm ± SEM (n=4). Significance tested with a one-way ANOVA with Bonferroni post-hoc analysis. * p<0.05, ** p<0.01, *** p<0.001, highlighted in bold.

Ligand	ΔT_M (°C)			
	c-MycC27	c-MycC52	c-MycG27	c-MycG52
PTN	0±0.5 0±0.5	-1±0.5 **-2±0.3***	-1±0.5	**+2±0.3***
VSE	0±0.6 -1±0.6	**-3±0.2**** **-14±0.5*****	-1±0.5	**+4±0.1****

In contrast, Pep-PTN caused a modest, 2±0.3°C decrease in T_M (p<0.05) of the more stable iM population with no significant change to lower T_M value. The complementary c-MycG52 sequence was modestly stabilized by both Pep-PTN (+2°C, p<0.05) and Pep-VSE (+4°C, p<0.01**) (Table 2 & Fig. S4B). To the best of our knowledge these are the first examples of ligands to target the long c-MycC sequence. There are a few ligands that have been found to target shorter versions of the sequence. For example, Li *et. al.* developed compound B19 which was found to stabilize the shorter c-MycC27 sequence (ΔT_M 11.5 °C),[33] Saha *et. al.* found a compound that stabilized a 33-mer variant of c-Myc (ΔT_M 29.7 °C)[34] and Debnath *et. al.* found a compound that stabilized the same sequence with a ΔT_M value of 32 °C.[35] Porzio *et. al.*[36] examined compounds against a 22-mer version and their best compound against that sequence of c-Myc showed a ΔT_M of −27.5 °C. To the best of our knowledge, Pep-VSE here is unique in destabilizing the long, biologically relevant, sequence from c-Myc.

The profound iM-destabilizing behavior of these peptides prompted us to examine if they could modulate gene expression in cells. The widely used Del-4 c-Myc promoter reporter construct was selected to investigate the biological effects of the peptide delivery into cells. The large molecular mass (>1500 g/mole) of the peptides at physiological pH prompted us to use Nanocin Pro® to enhance cellular uptake. Relative c-Myc promoter activity was measured in a dual reporter gene assay by normalizing Firefly expression, which is proportional to c-Myc expression, and *Renilla* luciferase expression as an internal control (Fig. 2A). Treatment with Pep-PTN caused a concentration-dependent increase in luciferase activity up to a 16-36% increase across a 1-10 µM range (p<0.001 - 0.01) compared to the vehicle only control (Nanocin Pro + 0.2% DMSO). By contrast, delivery of Pep-VSE significant decreased c-Myc promoter-driven luciferase activity by 36 ± 1.8% at 10 µM concentrations (p<0.001). Cell viability assays were conducted concurrently with the luciferase assays (Fig. 2B). No significant changes to cell viability were observed, indicating that the modulated luciferase levels were not due to peptide-mediated changes in cell viability.

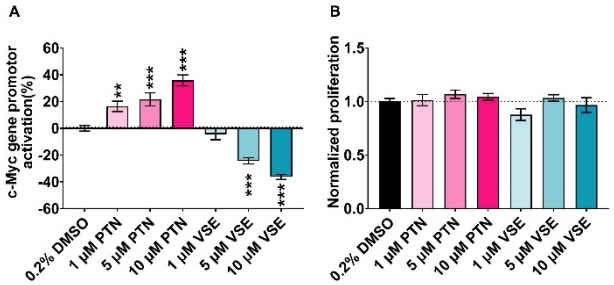

Figure 2. Dual reporter gene assay (A) and MTS assay (B) in HEK293 cells transfected with reporter plasmid including 52 bp long c-Myc sequence regulating firefly luciferase and normalized to control *Renilla* luciferase signal. The assays were performed after 4h of treatment with DMSO, Pep-PTN or Pep-VSE and normalized to DMSO control. Data shown are mean ± SEM (n=6), * $p<0.05$, ** $p<0.01$, *** $p<0.001$ determined by a one-way ANOVA with Bonferroni post-hoc analysis.

In this study we identified two selective peptide ligands for the c-MycC52 iM sequence. Our data demonstrated that the ability of Pep-PTN to destabilize c-MycC52 equaled its stabilization of c-MycG52, according to CD melting analysis. Whereas, Pep-VSE had a large destabilization effect on c-MycC52 that far exceeded its subtle cMycG52 stabilization. Hurley and co-workers illuminated the mutually exclusive binding of nucleolin and hnRNP-K to the c-Myc G quadruplex and i-motif structures, and highlighted the challenge in the design of chemical probes and drug molecules that can precisely control c-Myc transcriptional firing. Aberrant activation of c-Myc transcription has the potential to further promote cancer cell growth. The only other peptides that have been studied to target i-motif were targeting Hif-1-α and these were not assessed for their potential biological activity.[37]

Here, we report two peptidic ligands with demonstrable capacity to module c-Myc transcription in intact cells. These could be useful tools for studying c-Myc gene expression or may act as lead compounds for development of peptidomimetic therapeutics targeting c-Myc with enhanced drug-like properties.

Data Availability

All data will be available at 10.5281/zenodo.14258360.

Acknowledgements

Author contributions: ‡These authors contributed equally.

Corresponding Author

Zoë Waller (z.waller@ucl.ac.uk) and Christopher Morris chris.morris@ucl.ac.uk)

Funding

This work was supported by the BBSRC Norwich Research Park Biosciences Doctoral Training Partnership (grant number BB/M011216/1 – studentship for S.R.). D.G. was supported by the BBSRC (BB/W001616/1).

References

(1) Gehring, K.; Leroy, J.-L.; Guéron, M. A tetrameric DNA structure with protonated cytosine-cytosine base pairs. *Nature* **1993**, *363* (6429), 561-565. DOI: 10.1038/363561a0.
(2) Day, H. A.; Pavlou, P.; Waller, Z. A. E. i-Motif DNA: Structure, stability and targeting with ligands. *Bioorganic & Medicinal Chemistry* **2014**, *22* (16), 4407-4418. DOI: https://doi.org/10.1016/j.bmc.2014.05.047.
(3) Zhou, J.; Wei, C.; Jia, G.; Wang, X.; Feng, Z.; Li, C. Formation of i-motif structure at neutral and slightly alkaline pH. *Molecular BioSystems* **2010**, *6* (3), 580-586, 10.1039/B919600E. DOI: 10.1039/B919600E.
(4) Wright, E. P.; Huppert, J. L.; Waller, Z. A. E. Identification of multiple genomic DNA sequences which form i-motif structures at neutral pH. *Nucleic acids research* **2017**, *45* (6), 2951-2959. DOI: 10.1093/nar/gkx090 From NLM Medline.
(5) Zeraati, M.; Langley, D. B.; Schofield, P.; Moye, A. L.; Rouet, R.; Hughes, W. E.; Bryan, T. M.; Dinger, M. E.; Christ, D. I-motif DNA structures are formed in the nuclei of human cells. *Nature Chemistry* **2018**, *10* (6), 631-637. DOI: 10.1038/s41557-018-0046-3.

(6) King, J. J.; Irving, K. L.; Evans, C. W.; Chikhale, R. V.; Becker, R.; Morris, C. J.; Pena Martinez, C. D.; Schofield, P.; Christ, D.; Hurley, L. H.; et al. DNA G-Quadruplex and i-Motif Structure Formation Is Interdependent in Human Cells. *J Am Chem Soc* **2020**, *142* (49), 20600-20604. DOI: 10.1021/jacs.0c11708 From NLM Medline.
(7) Zanin, I.; Ruggiero, E.; Nicoletto, G.; Lago, S.; Maurizio, I.; Gallina, I.; Richter, S. N. Genome-wide mapping of i-motifs reveals their association with transcription regulation in live human cells. *Nucleic Acids Research* **2023**, *51*, 8309 - 8321.
(8) Dhanasekaran, R.; Deutzmann, A.; Mahauad-Fernandez, W. D.; Hansen, A. S.; Gouw, A. M.; Felsher, D. W. The MYC oncogene - the grand orchestrator of cancer growth and immune evasion. *Nat Rev Clin Oncol* **2022**, *19* (1), 23-36. DOI: 10.1038/s41571-021-00549-2 From NLM.
(9) Dang, C. V. MYC on the path to cancer. *Cell* **2012**, *149* (1), 22-35. DOI: 10.1016/j.cell.2012.03.003 From NLM Medline.
(10) Jain, M.; Arvanitis, C.; Chu, K.; Dewey, W.; Leonhardt, E.; Trinh, M.; Sundberg, C. D.; Bishop, J. M.; Felsher, D. W. Sustained loss of a neoplastic phenotype by brief inactivation of MYC. *Science* **2002**, *297* (5578), 102-104. DOI: 10.1126/science.1071489 From NLM.
(11) Jung, L. A.; Gebhardt, A.; Koelmel, W.; Ade, C. P.; Walz, S.; Kuper, J.; von Eyss, B.; Letschert, S.; Redel, C.; d'Artista, L.; et al. OmoMYC blunts promoter invasion by oncogenic MYC to inhibit gene expression characteristic of MYC-dependent tumors. *Oncogene* **2017**, *36* (14), 1911-1924. DOI: 10.1038/onc.2016.354 From NLM.
(12) Soucek, L.; Whitfield, J. R.; Sodir, N. M.; Massó-Vallés, D.; Serrano, E.; Karnezis, A. N.; Swigart, L. B.; Evan, G. I. Inhibition of Myc family proteins eradicates KRas-driven lung cancer in mice. *Genes Dev* **2013**, *27* (5), 504-513. DOI: 10.1101/gad.205542.112 From NLM.
(13) Esain-Garcia, I.; Kirchner, A.; Melidis, L.; Tavares, R. C. A.; Dhir, S.; Simeone, A.; Yu, Z.; Madden, S. K.; Hermann, R.; Tannahill, D.; Balasubramanian, S. G-quadruplex DNA structure is a positive regulator of MYC transcription. *Proc Natl Acad Sci U S A* **2024**, *121* (7), e2320240121. DOI: 10.1073/pnas.2320240121 From NLM Medline.
(14) Rudolph, C.; Adam, G.; Simm, A. Determination of Copy Number of c-Myc Protein per Cell by Quantitative Western Blotting. *Analytical Biochemistry* **1999**, *269* (1), 66-71. DOI: https://doi.org/10.1006/abio.1999.3095.
(15) Dani, C.; Blanchard, J. M.; Piechaczyk, M.; El Sabouty, S.; Marty, L.; Jeanteur, P. Extreme instability of myc mRNA in normal and transformed human cells. *Proceedings of the National Academy of Sciences* **1984**, *81* (22), 7046-7050. DOI: doi:10.1073/pnas.81.22.7046.
(16) Wierstra, I.; Alves, J. The c□myc Promoter: Still MysterY and Challenge. In *Advances in Cancer Research*, Vol. 99; Academic Press, 2008; pp 113-333.
(17) Davis, T. L.; Firulli, A. B.; Kinniburgh, A. J. Ribonucleoprotein and protein factors bind to an H-DNA-forming c-myc DNA element: possible regulators of the c-myc gene. *Proceedings of the National Academy of Sciences* **1989**, *86* (24), 9682-9686. DOI: doi:10.1073/pnas.86.24.9682.
(18) Berberich, S. J.; Postel, E. H. PuF/NM23-H2/NDPK-B transactivates a human c-myc promoter-CAT gene via a functional nuclease hypersensitive element. *Oncogene* **1995**, *10* (12), 2343-2347. PubMed.
(19) Dai, J.; Hatzakis, E.; Hurley, L. H.; Yang, D. I-motif structures formed in the human c-MYC promoter are highly dynamic--insights into sequence redundancy and I-motif stability. *PLoS One* **2010**, *5* (7), e11647. DOI: 10.1371/journal.pone.0011647 From NLM.
(20) Grand, C. L.; Han, H.; Muñoz, R. M.; Weitman, S.; Von Hoff, D. D.; Hurley, L. H.; Bearss, D. J. The cationic porphyrin TMPyP4 down-regulates c-MYC and human telomerase reverse transcriptase expression and inhibits tumor growth in vivo. *Mol Cancer Ther* **2002**, *1* (8), 565-573. From NLM.
(21) Siddiqui-Jain, A.; Grand, C. L.; Bearss, D. J.; Hurley, L. H. Direct evidence for a G-quadruplex in a promoter region and its targeting with a small molecule to repress c-MYC transcription. *Proc Natl Acad Sci U S A* **2002**, *99* (18), 11593-11598. DOI: 10.1073/pnas.182256799 From NLM.
(22) Yang, D.; Hurley, L. H. Structure of the biologically relevant G-quadruplex in the c-MYC promoter. *Nucleosides Nucleotides Nucleic Acids* **2006**, *25* (8), 951-968. DOI: 10.1080/15257770600809913 From NLM.
(23) Brooks, T. A.; Hurley, L. H. The role of supercoiling in transcriptional control of MYC and its importance in molecular therapeutics. *Nature Reviews Cancer* **2009**, *9* (12), 849-861. DOI: 10.1038/nrc2733.
(24) Sekibo, D. A. T.; Fox, K. R. The effects of DNA supercoiling on G-quadruplex formation. *Nucleic Acids Res* **2017**, *45* (21), 12069-12079. DOI: 10.1093/nar/gkx856 From NLM.
(25) Brown, S. L.; Kendrick, S. The i-Motif as a Molecular Target: More Than a Complementary DNA Secondary Structure. *Pharmaceuticals* **2021**, *14* (2), 96.
(26) Sutherland, C.; Cui, Y.; Mao, H.; Hurley, L. H. A Mechanosensor Mechanism Controls the G-Quadruplex/i-Motif Molecular Switch in the MYC Promoter NHE III(1). *J Am Chem Soc* **2016**, *138* (42), 14138-14151. DOI: 10.1021/jacs.6b09196 From NLM.
(27) Zhou, W.; Jie, Q.; Pan, T.; Shi, J.; Jiang, T.; Zhang, Y.; Ding, N.; Xu, J.; Ma, Y.; Li, Y. Single-cell RNA binding protein regulatory network analyses reveal oncogenic HNRNPK-MYC signalling pathway in cancer. *Commun Biol* **2023**, *6* (1), 82. DOI: 10.1038/s42003-023-04457-2 From NLM.
(28) Anthis, N. J.; Clore, G. M. Sequence-specific determination of protein and peptide concentrations by absorbance at 205 nm. *Protein Sci* **2013**, *22* (6), 851-858. DOI: 10.1002/pro.2253 From NLM Medline.
(29) Sheng, Q.; Neaverson, J. C.; Mahmoud, T.; Stevenson, C. E. M.; Matthews, S. E.; Waller, Z. A. E. Identification of new DNA i-motif binding ligands through a fluorescent intercalator displacement assay. *Org Biomol Chem* **2017**, *15* (27), 5669-5673. DOI: 10.1039/c7ob00710h From NLM Medline.
(30) Liu, K. C.; Röder, K.; Mayer, C.; Adhikari, S.; Wales, D. J.; Balasubramanian, S. Affinity-Selected Bicyclic Peptide G-Quadruplex Ligands Mimic a Protein-like Binding Mechanism. *J Am Chem Soc* **2020**, *142* (18), 8367-8373. DOI: 10.1021/jacs.0c01879 From NLM.
(31) DesJardins, E.; Hay, N. Repeated CT elements bound by zinc finger proteins control the absolute and relative activities of the two principal human c-myc promoters. *Mol Cell Biol* **1993**, *13* (9), 5710-5724. DOI: 10.1128/mcb.13.9.5710-5724.1993 From NLM.
(32) Dexheimer, T. S.; Carey, S. S.; Zuohe, S.; Gokhale, V. M.; Hu, X.; Murata, L. B.; Maes, E. M.; Weichsel, A.; Sun, D.; Meuillet, E. J.; et al. NM23-H2 may play an indirect role in transcriptional activation of c-myc gene expression but does not cleave the nuclease hypersensitive element III(1). *Mol Cancer Ther* **2009**, *8* (5), 1363-1377. DOI: 10.1158/1535-7163.MCT-08-1093 From NLM Medline.
(33) Shu, B.; Cao, J.; Kuang, G.; Qiu, J.; Zhang, M.; Zhang, Y.; Wang, M.; Li, X.; Kang, S.; Ou, T.-M.; et al. Syntheses and evaluation of new acridone derivatives for selective binding of oncogene c-myc promoter i-motifs in gene transcriptional regulation. *Chemical Communications* **2018**, *54* (16), 2036-2039, 10.1039/C8CC00328A. DOI: 10.1039/C8CC00328A.
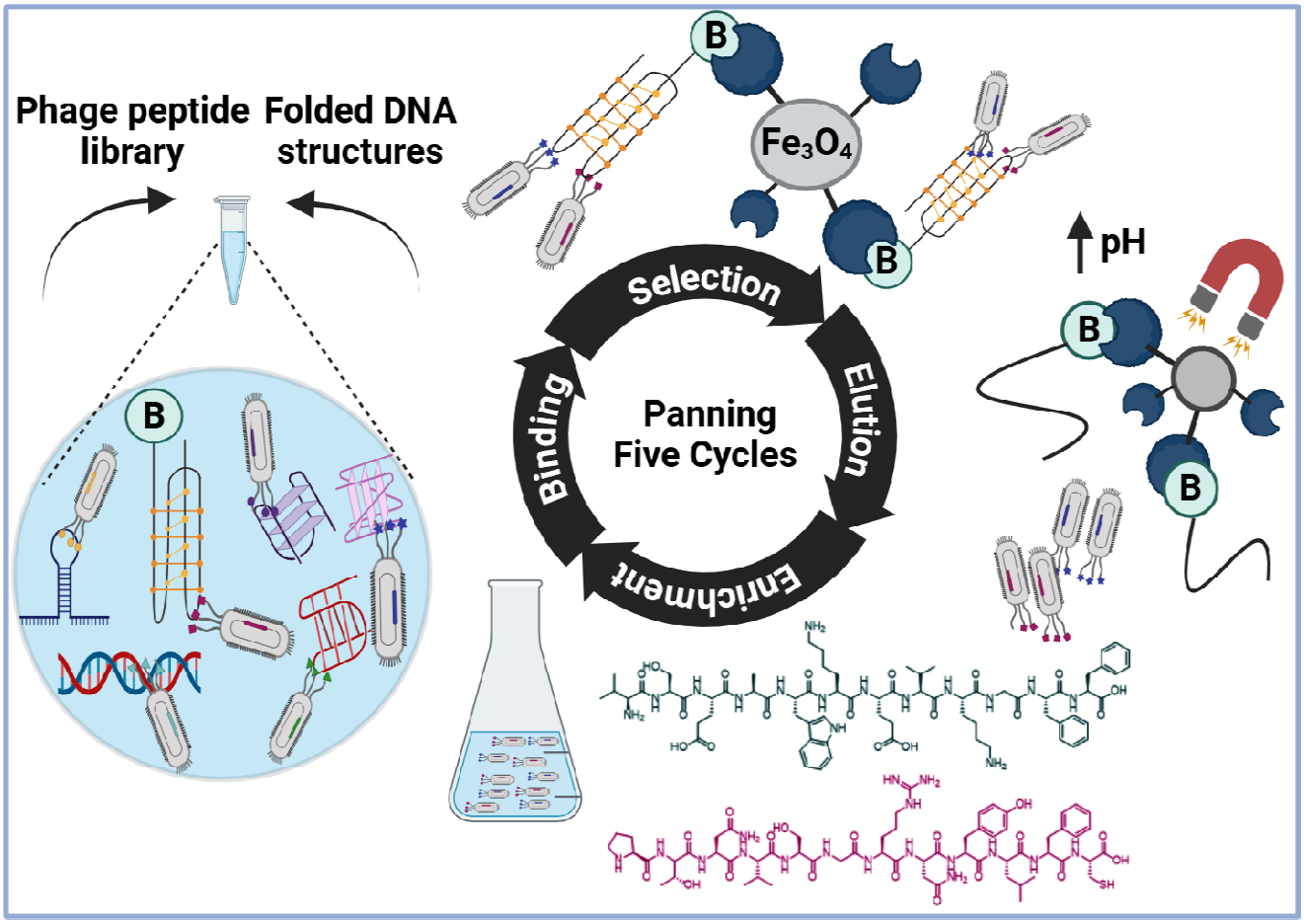
(34) Saha, P.; Panda, D.; Müller, D.; Maity, A.; Schwalbe, H.; Dash, J. In situ formation of transcriptional modulators using non-canonical DNA i-motifs. *Chemical Science* **2020**, *11* (8), 2058-2067, 10.1039/D0SC00514B. DOI: 10.1039/D0SC00514B.
(35) Debnath, M.; Ghosh, S.; Chauhan, A.; Paul, R.; Bhattacharyya, K.; Dash, J. Preferential targeting of i-motifs and G-quadruplexes by small molecules. *Chemical Science* **2017**, *8* (11), 7448-7456, 10.1039/C7SC02693E. DOI: 10.1039/C7SC02693E.
(36) Di Porzio, A.; Galli, U.; Amato, J.; Zizza, P.; Iachettini, S.; Iaccarino, N.; Marzano, S.; Santoro, F.; Brancaccio, D.; Carotenuto, A.; et al. Synthesis and Characterization of Bis-Triazolyl-Pyridine Derivatives as Noncanonical DNA-Interacting Compounds. *International Journal of Molecular Sciences* **2021**, *22* (21), 11959.
(37) Ghosh, D.; Pratihar, S.; Govindaraju, T. Designer tryptophan-rich peptide modulates structural dynamics of HIF-1α DNA i-motif DNA. *Journal of Peptide Science* **2024**, *30* (8), e3601. DOI: https://doi.org/10.1002/psc.3601.